Photophysics of PTCDA and Me-PTCDI Thin Films: Effects of Growth Temperature

A. J. Ferguson and T. S. Jones*

Centre for Electronic Materials and Devices, Department of Chemistry, Imperial College London, South Kensington, London SW7 2AZ, United Kingdom

Received: November 28, 2005

The effect of deposition temperature on the photophysical properties of 3,4,9,10-perylenetetracarboxylic dianhydride (PTCDA) and *N*,*N*′-dimethylperylene-3,4,9,10-bis(dicarboximide) (Me-PTCDI) films is investigated with steady-state and time-resolved spectroscopy. Atomic force microscopy (AFM) images of the film surfaces show an increase in the dimensions of crystallites with substrate temperature, culminating in the formation of elongated crystallites on substrates held close to the sublimation temperature. In contrast, despite an improvement in the crystal quality, X-ray diffraction (XRD) studies indicate that the substrate temperature has a negligible effect on the molecular orientation; the PTCDA and Me-PTCDI molecules align parallel and tilted to the substrate surface, respectively. Both materials exhibit characteristic absorption, due to mixing between charge-transfer and Frenkel species, and broad structureless photoluminescence. Growth at elevated temperatures gives rise to increased low-energy absorption, attributed to the formation of charge-transfer species, and enhanced blue-shifted emission, although the effects are less pronounced for Me-PTCDI. Time-correlated single-photon counting data indicate that the enhancement coincides with a lengthening of the fluorescence decays, over the whole emission spectrum.

1. Introduction

The unique electronic and optical properties, coupled with the flexibility and tunability in processing, have driven the considerable interest in vapor deposited thin films of molecular-based semiconductor materials over the past few decades.[1] Various perylenetetracarboxylic acid derivatives, such as PTCDA (perylene-3,4,9,10-tetracarboxylic dianhydride) and Me-PTCDI (*N*,*N*′-dimethylperylene-3,4,9,10-bis(dicarboximide)), have been studied extensively and incorporated into photovoltaic[2,3] and photodetector[4,5] devices. However, despite the wide use of this class of materials, significant effort is still employed to understand their fundamental electronic properties, but surprisingly only a few studies have concentrated on the impact of the growth conditions and any subsequent annealing processes.[6,7]

PTCDA is known to crystallize in two polymorphic forms, α and *β*, depending on the specific growth conditions, though their structures are very similar—both crystallizing in the monoclinic $P2_1/c$ space group.[8] Although both polymorphs coexist when deposited on alkali halide substrates maintained at high temperatures (200−260 °C),[6] recent studies suggest that films grown on quartz substrates consist only of the α-form.[7] Me-PTCDI also crystallizes in the monoclinic $P2_1/c$ space group, with two molecules per unit cell,[9] but unlike PTCDA no polymorphic forms have been identified. In both cases the molecules *π*-stack to form quasi-1D crystals,[10] with molecules in neighboring stacks adopting a herringbone arrangement. However, projection of the long axes of the molecules in neighboring stacks onto the (102) plane reveals that the axes are essentially orthogonal (PTCDA) and ∼36° (Me-PTCDI) to each other. Detailed structural studies of PTCDA deposited onto Si(100) and quartz reveal that the molecules are oriented with their planes approximately parallel (tilted between 10° and 15°) to the substrate surface.[11] By contrast, structural studies of Me-PTCDI deposited on ITO-coated glass revealed the presence of two diffraction peaks at ∼7.8° and 12.2°, associated with scattering from the (011) and (002) planes, respectively.[12] The dominant peak at 12.2° corresponds to a molecular orientation where the short axis is tilted by approximately 60° with respect to the substrate plane, so that the stacking and long molecular axes lie parallel to the substrate surface. More recent studies have also observed this molecular arrangement, using variable angle spectroscopic ellipsometry and infrared reflection spectroscopy, for Me-PTCDI deposited on sulfur-passivated GaAs-(100) substrates.[13] The relative orientation of molecules, projected onto the (102) plane of the unit cell, in neighboring 1D-stacks is shown schematically in Figure 1 for α-PTCDA (a), *β*-PTCDA (b), and Me-PTCDI (c).

The morphological properties of the two thin film systems have also been reported for growth on different substrates. Room temperature deposition of Me-PTCDI on poly(ethylene terephthalate) (PETP) yields films consisting of approximately spherical crystallites, with lateral dimensions of ∼100 nm.[10] PTCDA films (on quartz) grown at room temperature are very smooth and consist of spherical crystallites of ∼50−100 nm, which become considerably elongated on substrates maintained close to the sublimation temperature, giving rise to a significant roughening of the film surface.[7]

Several experimental and theoretical studies have used the crystal structures of PTCDA and Me-PTCDI to rationalize the observed electronic properties in the solid state.[14−18] Despite these efforts the precise nature of the optical species present in the solid state has become a source of intense debate. It is generally accepted that the electronic absorption spectrum of PTCDA and Me-PTCDI films originates from both monomeric transitions and excitations to a low-energy state.[19] Although Raman studies suggest that optical absorption cannot lead

* To whom correspondence should be addressed. Phone: +44 (0) 20 7594 5794. Fax: +44 (0) 20 7594 5801. E-mail: t.jones@imperial.ac.uk.

10.1021/jp056899u CCC: $33.50
Published on Web 03/09/2006

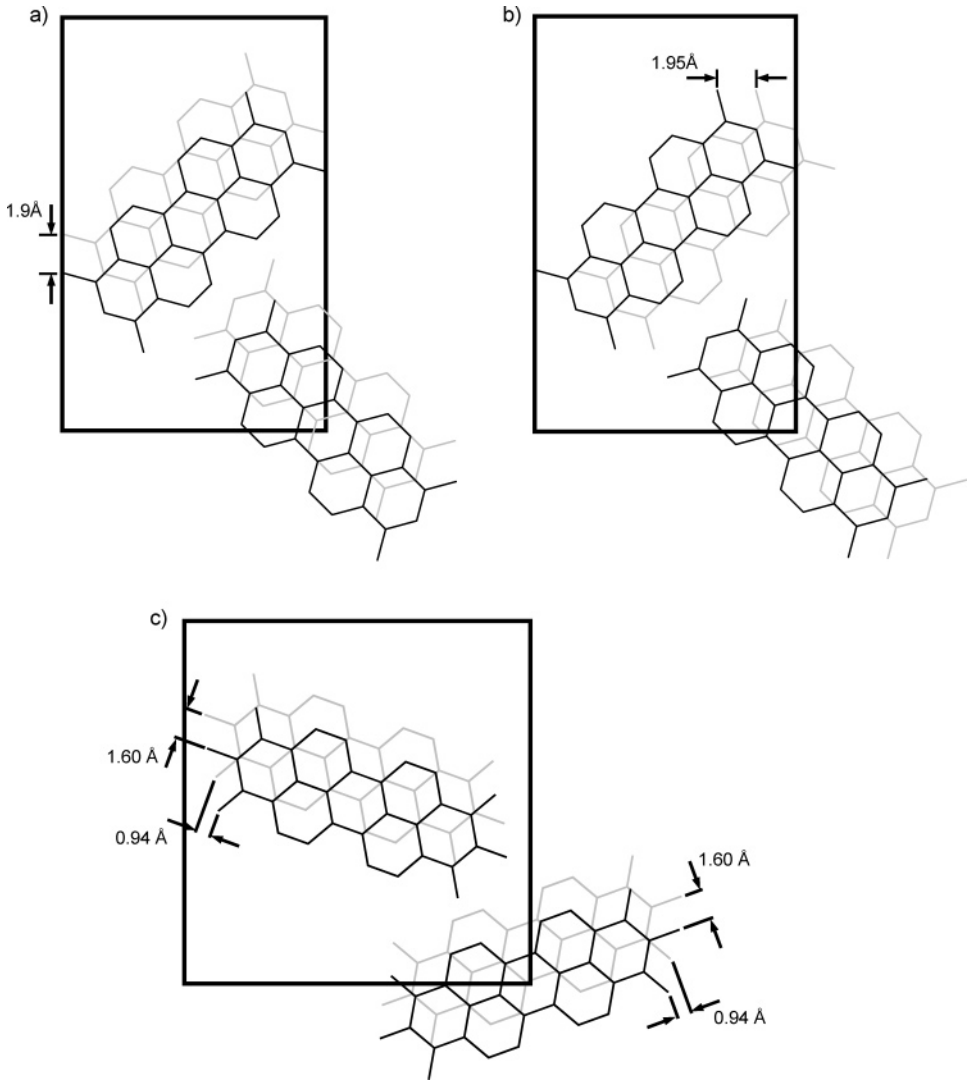

Figure 1. Schematic showing the arrangement of molecules in two adjacent (102) planes for (a) α-PTCDA, (b) *β*-PTCDA, and (c) Me-PTCDI: the molecules in the lattice are drawn in black, and the molecules in the adjacent unit cell in gray.

directly to charge separation,[20] the low-energy state has been attributed to various species involving molecular ionization, for example charge transfer[14] or Wannier−Mott[21] excitons. More recent theoretical studies employ a mixture of Frenkel (FE) and charge-transfer (CT) contributions to describe the absorption of light.[16−18] Although the models require a significant degree of complexity to fully account for experimental results, they are capable of describing the polarization dependence and electroabsorption characteristics.

Initial studies of the nature of the excited states in crystalline PTCDA and Me-PTCDI films attributed the observed photoluminescence (PL) to two emissive components.[22] The high-energy emission was attributed to a monomer-like species and the broad red-shifted emission to two excimeric states; for both materials the excimeric species are longer lived than the monomer. However, more recent time-resolved PL studies of solid-state PTCDA have discovered that the kinetic scheme for radiative relaxation from the excited states required five spectral components to accurately describe the overall emission. These components have been attributed to Frenkel (thought to be due to emission from the relaxed CT-FE species), excimer (due to two excimeric species) and charge-transfer species, with the addition of S-band, and high-energy states—the latter have been attributed as emission from the relaxed monomer species or crystal defects.[23−25] Recent theoretical calculations of the energies for all possible excited-state species have reassigned the CT and S-band emissive components as self-trapped charge-transfer species, with different geometries.[25,26]

In this paper we present XRD, AFM, and both steady-state and time-resolved spectroscopic data for PTCDA and Me-PTCDI films grown on quartz substrates at various temperatures. The structural and morphological results confirm an increase in the size and quality of the observed crystallites with growth temperature, while the spectroscopic studies suggest that these structural changes result in increased absorption due to charge-transfer species and enhanced emission, particularly from high-energy species.

2. Experimental Details

The films were prepared at a pressure of 10^{-9} Torr in an ultrahigh vacuum (UHV) chamber equipped with Knudsen cells loaded with PTCDA (Fluka) and Me-PTCDI (SynTec-Sensient) powders, which were used after double purification by gradient sublimation. The purified powders were outgassed under vacuum for 1 h prior to deposition, and evaporated from sources held between 340 and 360 °C, corresponding to a growth rate of ∼2.5 Å/s, as determined by a quartz crystal microbalance positioned near the substrate. The films are 100 nm thick unless otherwise stated. The films were grown on quartz substrates

(Newcastle Optical Engineering), which were cleaned in a methanol sonic bath, and dried under a stream of dry nitrogen.

Surface morphology studies were performed with an atomic force microscope (Burleigh Instruments Metis-2000) operated in a noncontact (tapping) mode, and the structure of the films was determined with a powder X-ray diffractometer (Siemens D5000) with a Cu Kα source operating in the $\theta-2\theta$ mode between 5 and 30°.

Electronic absorption spectra were collected with a UV/vis spectrophotometer (Perkin-Elmer Lambda 2), while photoluminescence emission (PL) data, following excitation at 425 nm, were obtained on a fluorimeter (JY Horiba-Spex FluoroMax). A sample holder was adapted to allow illumination of the films perpendicular to the film surface. The emission was collected over an angle of between 15° and 35° to the incident light beam, and directed to the detector by two mirrors.

Fluorescence decays were measured by using the time-correlated single photon counting (TCSPC) technique. Excitation was provided by an electronically driven laser diode system (IBH NanoLED) at 404 nm, producing a 1 MHz pulse train, with each pulse having a temporal fwhm of ~200 ps. The subsequent emission is detected perpendicular to the excitation beam by a microchannel plate photomultiplier tube (Hamamatsu R3809U), a wideband amplifier (Research Communications Model 9009), a constant fraction timing discriminator (EG&G Ortec Model 584), a time-to-amplitude converter (Tennelec TC864), which was operated in reverse mode, and a multichannel pulse-to-height analyzer (EG&G/Perkin-Elmer Ortec Trump Card). Emission wavelength selection was provided by means of interference filters, providing a band-pass fwhm of ~15 nm. Fluorescence decays were collected to between 10 000 and 20 000 counts in the channel of maximum intensity.

3. Results and Discussion

3.1. Film Structure and Morphology. The morphology of PTCDA and Me-PTCDI films grown on quartz substrates held at ambient temperature is characterized by small, spherical crystallites, with a root-mean-square (rms) roughness (Rq) of 2.73 and 9.52 nm, for PTCDA and Me-PTCDI, respectively. The AFM images in Figure 2 (a and b) show that the crystallite dimensions are more uniform in PTCDA films, and that the observed crystallites in the Me-PTCDI film (50−150 nm) are, on average, larger than those observed for PTCDA (50−100 nm). This accounts for the increased roughness and suggests there is improved crystallinity in the Me-PTCDI films.

Film growth at elevated temperatures has a marked effect on the roughness of PTCDA and Me-PTCDI films, with the Rq value increasing to ~19 nm for films of both materials deposited at 240 °C. The origin for the increase in surface roughness can be seen in more detail in the AFM images in Figure 2 (panels c and d), where it is clear that the dimensions of the crystallites increase with deposition temperature. The PTCDA film grown at 240 °C (Figure 2c) consists of approximately spherical crystallites with lateral dimensions of 100−200 nm, consistent with previous reports.[7] By contrast, the features observed in Me-PTCDI films grown at 240 °C (Figure 2d) are randomly oriented and elongated, with lengths between 200 and 750 nm.

Although the same morphological trends are observed for films of both materials the crystallites in Me-PTCDI films are larger than those in the corresponding PTCDA films. It should also be noted that the transition from spherical to elongated crystallites appears to occur at lower temperatures for Me-PTCDI than PTCDA, which may be an indication of the ease of crystal formation for the dicarboximide derivative.

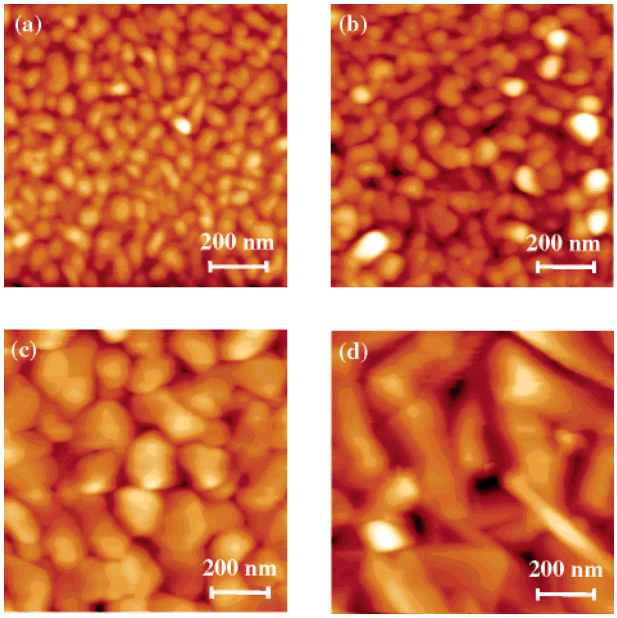

Figure 2. AFM images of 100 nm thick PTCDA films grown at (a) room temperature and (c) 240 °C and 100 nm thick Me-PTCDI films grown at (b) room temperature and (d) 240 °C.

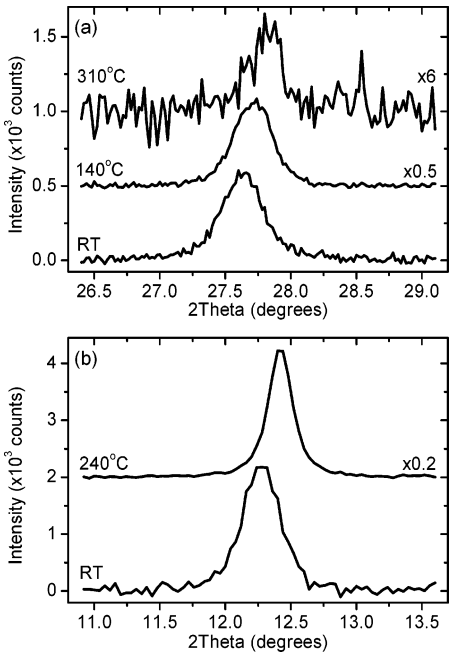

Figure 3. XRD 2θ scans for 100 nm thick (a) PTCDA and (b) Me-PTCDI films grown on quartz substrates held at various temperatures (partial sublimation of the PTCDA film grown at 310 °C accounts for the reduction in the intensity of the diffraction peak).

Powder XRD patterns for 100 nm thick PTCDA and Me-PTCDI films grown at various temperatures (Figure 3) illustrate the most intense bands for the two materials. For room-temperature growth the single peak at 2θ ~27.7° for PTCDA (a) corresponds to diffraction from the (102) plane of the α-polymorph,[11] and indicates that the molecules orient themselves approximately parallel to the surface of the quartz substrate and stack in successive layers with their planes parallel to each other. The peak observed at 2θ ~12.3° in the Me-PTCDI (b) diffraction pattern obtained for growth at room temperature corresponds to scattering from the (002) plane, i.e., the

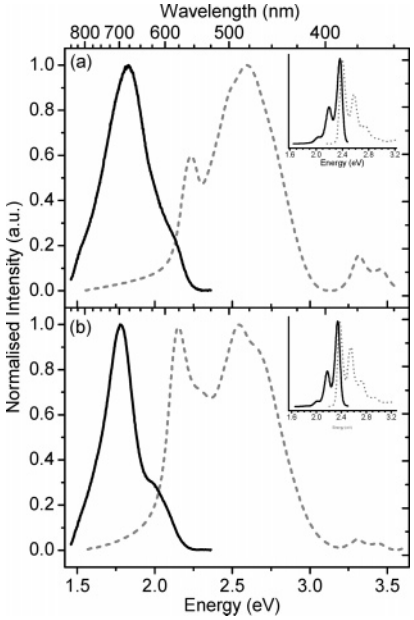

Figure 4. Normalized absorption (dashed lines) and photoluminescence (solid lines) spectra of 100 nm thick (a) PTCDA and (b) Me-PTCDI films grown at room temperature (the corresponding solution-phase absorption and emission spectra are shown in the insets).

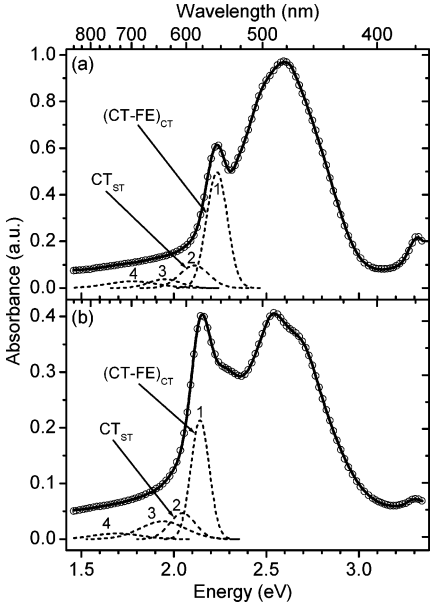

Figure 5. Contributions to the absorption of 100 nm (a) PTCDA and (b) Me-PTCDI films grown at room temperature: (1) CT-dominated CT-FE state, (2) self-trapped CT state, and (3 and 4) low-energy states. The data (○) and fit (solid line) are offset for clarity.

molecules are tilted at ∼60°, with the long molecular axes approximately parallel, to the substrate surface.[12] An additional peak, albeit much less intense, is also observed at ∼27.7° (not shown here), which corresponds to alignment of the molecular planes approximately parallel to the substrate surface.

The data in Figure 3 show a very small shift in the position of the diffraction peak for films of both materials grown at elevated temperatures. Although it is possible that the shift could be due to a contraction of the crystal lattice along the surface normal, resulting in a reduced *d* spacing between adjacent (102) and (002) planes for PTCDA and Me-PTCDI, respectively, it is more likely that it can be attributed to thickness and roughness differences and consequential variations in the alignment of the Cu Kα radiation with respect to the film surface, inducing a peak shift.[27] These results imply that the molecular orientation of both materials is essentially unaffected by growth at elevated temperatures.

Closer inspection of the diffraction data illustrates that initially the signal-to-noise ratio increases with growth temperature, indicating an improvement in the crystal size and quality, but decreases substantially when the substrate is held close to the deposition temperature, due to partial sublimation of the films. In addition, the increase in crystallite size at elevated temperatures gives rise to a decrease in the widths of the diffraction peaks, which is an indication of an increase in the size of the crystalline domains.

3.2. Photophysical Properties of Films Grown at Room Temperature. The electronic absorption spectra for (a) PTCDA and (b) Me-PTCDI films grown at room temperature (Figure 4) are significantly broadened with respect to the spectra obtained from isolated PTCDA and Me-PTCDI molecules (inset in Figure 4).

The absorption of both materials consists of a broad band at ∼2.5 eV (480 nm) and a sharp feature below 2.3 eV (>550 nm). As shown in Figure 5 it can be rationalized by using the charge-transfer-Frenkel (CT-FE) mixing model developed by Hoffmann et al.,[10,17] with the addition of a self-trapped CT state (Band 2),[14,15] and two low-energy bands (Bands 3 and 4), to account for the low-energy absorption tail. The broad band at ∼2.5 eV is of CT-FE origin, although it is dominated by a modified vibronic progression characteristic of the Frenkel exciton located on isolated molecules in solution. The fitting procedure involved using a sum of asymmetric Gaussian line shapes, which can best be described as a convolution of hypsochromic (blue-shifted) and bathochromic (red-shifted) Gaussian functions. Band asymmetry is more commonly employed to compensate for distortions caused by unresolved vibrational progressions.[28] However, in this case additional distortions could arise from coupling of the electronic state to more than one vibrational mode, variation in the extent of charge-transfer-Frenkel mixing in individual bands, variation in the extent of coupling to lattice vibrations (phonons), and Davydov splitting—in fact it is likely that all of these factors could be operating simultaneously.

Although a single self-trapped CT state was employed by Bulovic et al.,[14] to account for the low-energy absorption tail (no mention of self-trapped species was made by Hoffmann et al.), additional low-energy states were required to provide a good fit of the absorption in this study. These low-energy absorption features are likely to arise from additional "trap" geometries (stabilizing lattice deformations): the presence of several trap states has been observed for solid-state PTCDA[25] and perylene[29] (although these have mainly been observed in emission spectra).

The large Stokes shift observed between the maxima of the absorption and emission spectra (Figure 4) for PTCDA and Me-PTCDI films is indicative that the dominant absorbing and emitting species are either of different origin or there is significant relaxation of the excited-state species prior to emission. It should also be noted that the shape and position of the measured emission are independent of excitation wavelength (data not shown), contrary to studies of PTCDA films grown on quartz and KCl.[6]

The PL spectrum of the PTCDA film grown at room temperature, shown in Figure 4a, is blue-shifted with respect to the films studied by Scholz et al.[24] It is interesting to note that the absorption spectra measured in several independent studies are essentially identical, whereas the shape and position of the PL spectra often vary significantly, suggesting that

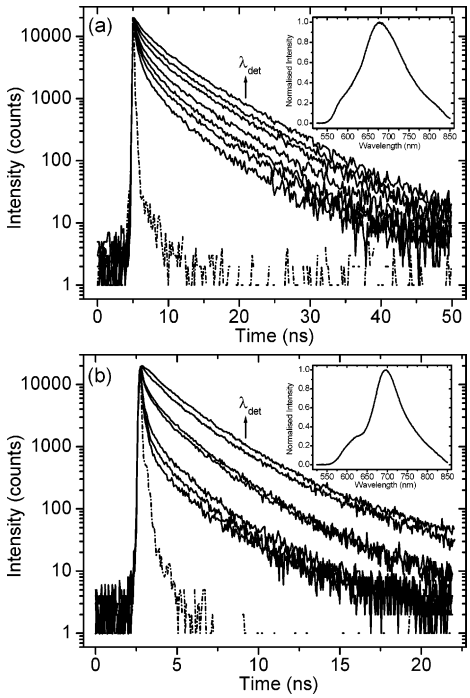

Figure 6. Fluorescence decays (solid lines) at 600, 630, 650, 670, 700, 770, and 815 nm, and instrument response function (dash-dotted line) for 100 nm thick (a) PTCDA and (b) Me-PTCDI films grown at room temperature (the corresponding PL spectra are shown in the insets).

relaxation from the excited states is more sensitive to the precise sample preparation, and that the observed differences are due to variations in the contribution of the individual species to the overall emission.

The PL spectra show almost no structure, with only a shoulder at the high-energy side of the main band, which is more pronounced for Me-PTCDI. Although the observed emission from PTCDA and Me-PCTDI is very similar, as would be expected, Figure 4 illustrates some clear differences. Most notably the emission bandwidth is significantly reduced for Me-PTCDI compared to PTCDA, suggesting that the improved crystallinity observed for Me-PTCDI films reduces the distribution of the excited states. This implies that structural defects may play some role in "trapping" the excited-state species, consistent with observations made for dimer formation in 9-cyanoanthracene,[30] and that an increase in the defect concentration results in a broadened distribution of excited states.

Fluorescence decays, recorded at different wavelengths across the emission spectrum, are presented in Figure 6. A distinct lengthening of the decay is observed for both 100 nm thick PTCDA and Me-PTCDI films, as the emission wavelength increases. Zahn and co-workers have performed several time-resolved PL studies of PTCDA single crystals and thin films which have illustrated the complexity of the emission from the relaxed excited states.[23−26] Global sum-of-exponential analysis indicates the presence of five decay lifetimes (for both PTCDA and Me-PTCDI), although the individual decays recorded at intervals across the emission spectrum are best described by tri- or tetraexponential kinetics, making it difficult to extract quantitative information about the emissive species.

The PL decays from PTCDA (a) films are considerably longer than those measured from Me-PTCDI (b), suggesting either that there are additional nonradiative pathways available to the excited-state energy or that the extent of quenching is greater in Me-PTCDI films. The fluorescence decays for both materials lengthen when detected at longer emission wavelengths, consistent with domination of the low-energy emission by excimeric species.

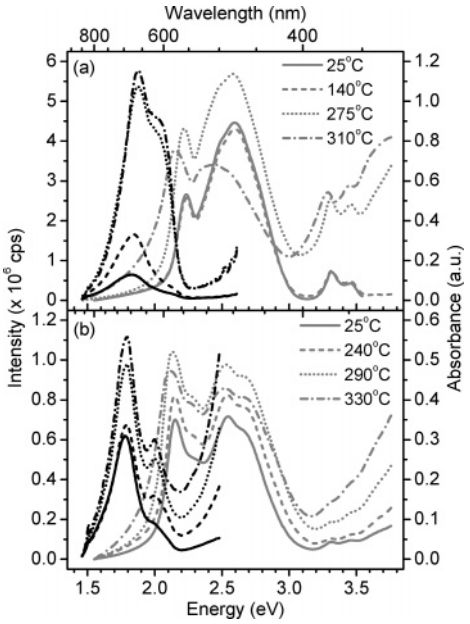

Figure 7. The effect of substrate temperature on the absorption (gray) and PL (black) spectra of (a) PTCDA and (b) Me-PTCDI films.

3.3. Photophysical Properties of Films Grown at Elevated Temperatures. The increase in the level of crystallinity and film roughness, observed in the powder XRD patterns and AFM images, respectively, is confirmed by the absorption and emission spectra of films grown at elevated temperatures (Figure 7). For both PTCDA and Me-PTCDI films, raising the substrate temperature causes more scattering in the ultraviolet region of the absorption spectrum, indicating that the film roughness is increasing. The PL spectra also display more scattering, in this case of the excitation source at 425 nm, with increasing growth temperature.

Comparison of the PTCDA and Me-PTCDI spectra shows that increasing the growth temperature has a greater effect on the optical properties of PTCDA, which could be due to a difference in the extent to which the crystallinity in the thin films is improved by elevation of the substrate temperature during growth.

Increasing the growth temperature of PTCDA from room temperature to 275 °C has little effect on the absorption spectrum, which retains the broad band at 2.6 eV (475 nm) and the sharp band at 2.2 eV (560 nm), except that the relative contribution of the sharp feature increases for films grown at 275 °C. However, for films deposited at 310 °C, which is just below the sublimation temperature, the absorption is significantly broadened and becomes dominated by the low-energy band.

The absorption of Me-PTCDI films shows a similar temperature dependence, with films grown between room temperature and 290 °C showing only a slight increase in the relative intensity of the sharp feature at 2.15 eV (575 nm). Again, the largest change in the absorption is observed for deposition close to the sublimation temperature (at 330 °C), where the low-energy features become much more dominant, causing significant broadening.

Although the precise nature of the PL measurement means that it is impossible to make a true quantitative comparison of the PL spectra, the emission is significantly enhanced in films grown at elevated temperatures. The enhancement is particularly evident for the high-energy shoulder, although the effect is much

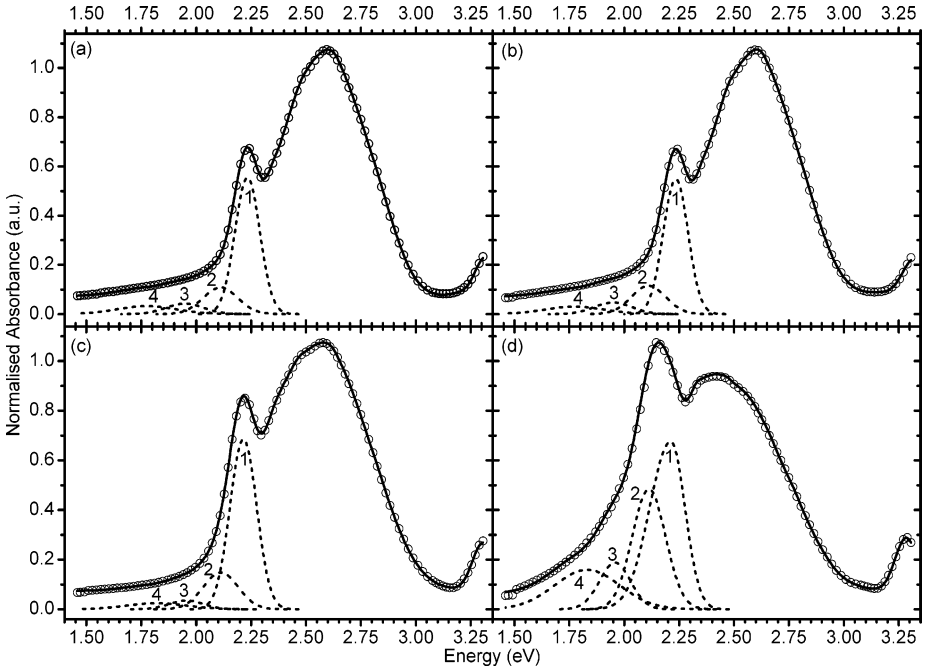

Figure 8. Contributions of the low-energy absorption components of PTCDA films grown at (a) room temperature, (b) 140 °C, (c) 275 °C, and (d) 310 °C. The data and fit curves are offset for clarity.

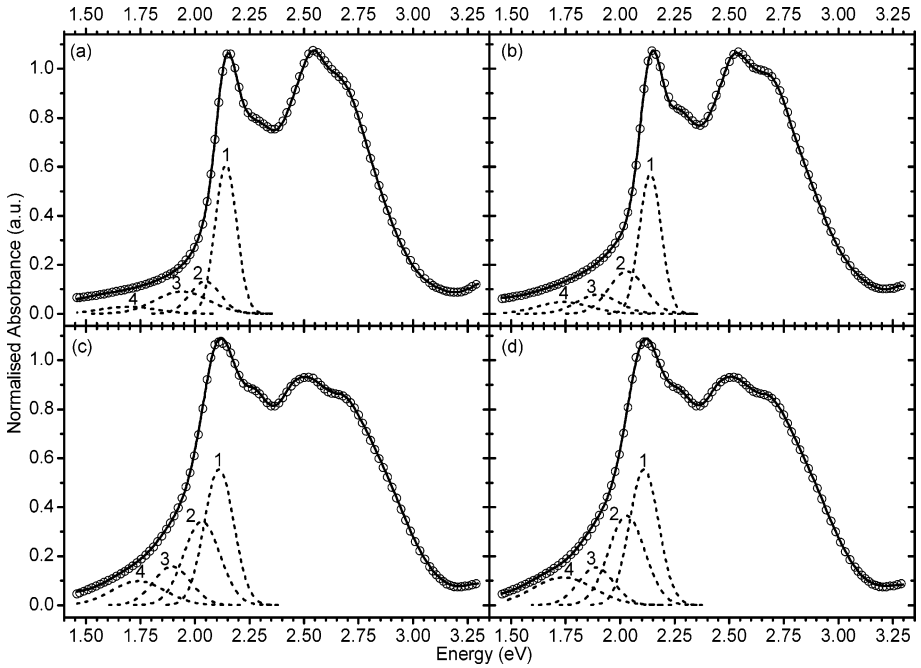

Figure 9. Contribution of the low-energy absorption components of Me-PTCDI films grown at (a) room temperature, (b) 240 °C, (c) 305 °C, and (d) 330 °. The data and fit curves are offset for clarity.

less pronounced in the case of Me-PTCDI, which is thought to be due to emissive species localized on individual molecules, supporting the suggestion that growth at elevated temperatures has a greater effect on the ordering in PTCDA films than Me-PTCDI.

These observations can be rationalized in terms of an increase in the contribution to the absorption by the charge-transfer (both free and self-trapped) and low-energy species. Figure 8 shows that PTCDA film growth at 140 °C has little effect on the contributions of the CT-FE and self-trapped CT states to the absorption. However, growth above 140 °C initially causes an increase in the contribution from the CT species, followed by a significant enhancement of the absorption due to the low-energy species, and subsequent broadening of the low-energy feature, at 310 °C.

Since the formation of charge-transfer species requires good orbital overlap between adjacent stacked molecules (uninterrupted ordering within the 1D stacks) the formation of these species, particularly those prone to self-trapping, will be dependent on crystal quality. Therefore, the absorption due to these species is likely to increase with elevation of the growth temperature, since improved crystal quality will remove defects, facilitating charge separation and increasing the number of sites favorable to the formation of charge-transfer species.

A similar trend is observed in the absorption of Me-PTCDI films grown at elevated temperatures (Figure 9), with a large

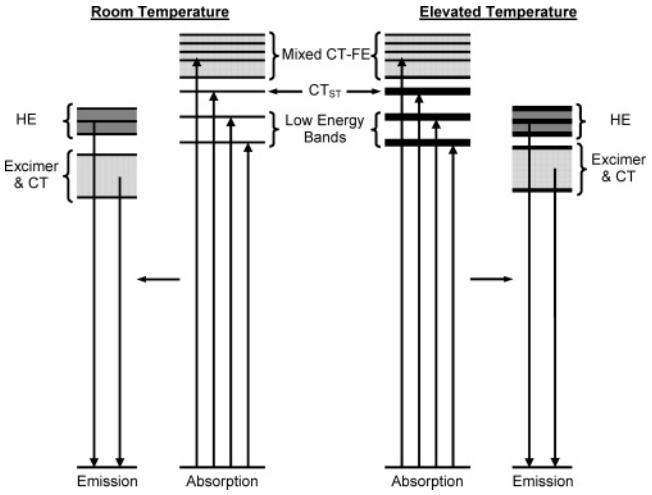

Figure 10. Schematic showing the effect of growth at elevated temperature on the absorption and emission from PTCDA and Me-PTCDI films.

increase in the contribution from the trapped charge-transfer and low-energy states. In addition, these absorption bands are slightly red-shifted, implying that the improvement in crystal quality improves the ability of lattice deformations to stabilize the excitation, causing an increase in the depth of trapping for these self-trapped CT species.

Although the relative contributions of the individual species will vary with growth temperature, the observed PL enhancement implies that the emission from all species is stronger. This is not entirely unexpected, since an improvement in the crystal quality will reduce the number of defects, both within the crystallites and at grain boundaries, capable of providing nonradiative deactivation pathways for the excitation. In addition, the increase in the crystallite dimensions will allow the excitonic species to diffuse further within the crystallites before encountering defect sites, or grain boundaries, which can provide nonradiative relaxation pathways for the exciton energy.

The blue-shift of the emission suggests that the reduction in the concentration of crystal defects, due to growth at elevated temperatures, removes the deep-traps for these excited-state species. This implies that stabilization of the excitonic species within these films may be provided by two mechanisms, (i) defect sites, which give rise to deeply trapped excitons and (ii) lattice deformations in good quality crystals that result in shallow-trapped excitons, and that the second mechanism dominates in films grown at elevated temperatures.

Photoluminescence excitation (PLE) measurements for PTCDA films grown on quartz indicate that the emission from films grown at elevated temperatures is dominated by excitation into the mixed CT-FE states, implying that the trapped CT species observed in the absorption spectra are only weakly fluorescent.[7]

In contrast to PTCDA, the emission observed from Me-PTCDI films has only a very slight dependence on the growth temperature (Figure 7). However, the contribution from the high-energy species is increased for growth on substrates held above room temperature.

Growth at elevated temperatures leads to a shift of the emission to higher energy, consistent with the observations made for PTCDA films grown at elevated temperatures, although the effect is much less pronounced.

Figure 10 shows the effect that growth at elevated temperatures has on the energy levels responsible for the absorption and emission spectra obtained from PTCDA and Me-PTCDI films. Our results show that only the absorption bands associated with a concomitant charge separation are enhanced for films grown at elevated temperature. Although the overall emission is enhanced, the effect is much more pronounced for the high-energy bands associated with monomer-like emission.

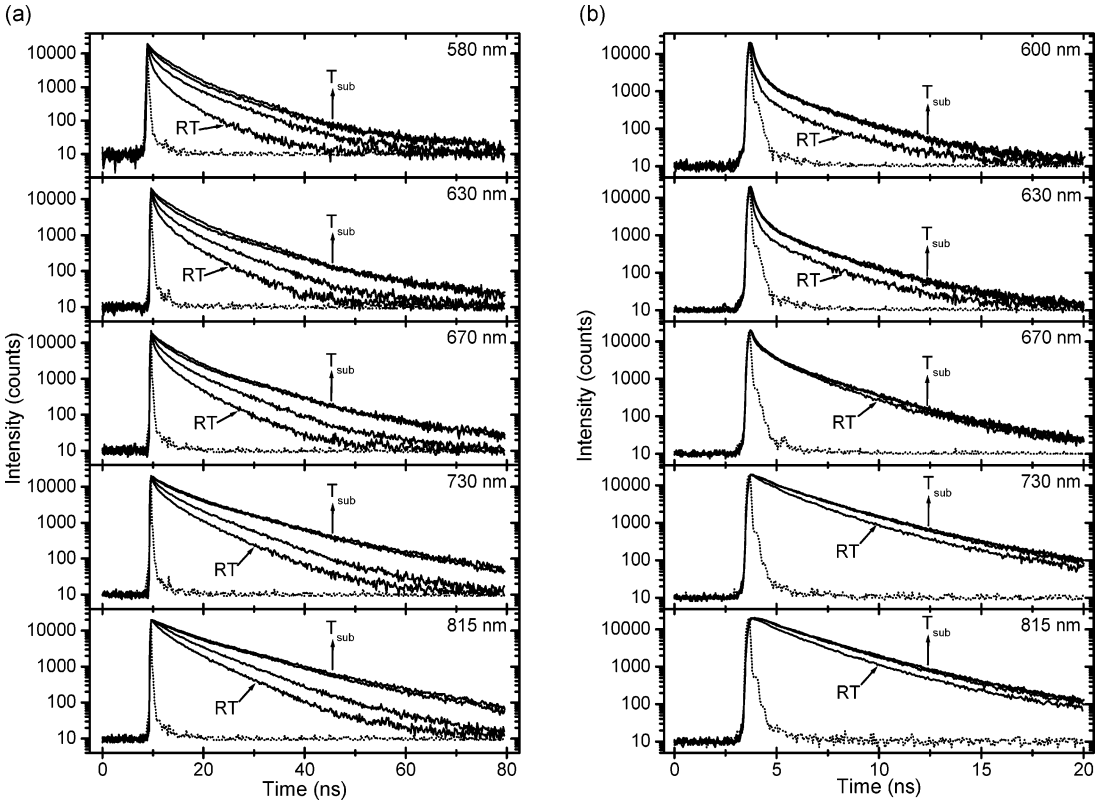

Figure 11. Evolution of the fluorescence decays (solid lines) with growth temperature for (a) PTCDA and (b) Me-PTCDI films, measured at different emission wavelengths; in each case the instrument response function (IRF) is indicated by the dotted line.

More information about the effect of growth temperature on the individual emissive species can be obtained from the fluorescence decays. The decays, measured at different points in the emission spectrum (Figure 11) for (a) PTCDA and (b) Me-PTCDI show that the decays lengthen (independent of the detection wavelength) as the growth temperature is increased, confirming that growth at elevated temperatures reduces nonradiative relaxation processes. Similar to the absorption and steady state, PL growth at elevated temperatures has a more pronounced effect on the kinetics of PTCDA films than for Me PTCDI.

4. Conclusion

It has been shown that the two perylene derivatives, PTCDA and Me-PTCDI, experience a significant increase in the strength of the intermolecular interactions when the materials are deposited as thin films. Deposition of both materials at room temperature results in films consisting of small spherical crystallites, with the molecules oriented parallel (PTCDA) and tilted (Me-PTCDI) with respect to the substrate surface. Crystal formation results in the generation of several new absorbing species, namely charge transfer (free and self-trapped) excitons and low-energy states, which are attributed to the strong orbital overlap experienced as a result of crystal formation. Crystal formation also gives rise to emissive species not observed in solution, such as excimers and charge-trapped species, and the analysis of the PL from PTCDA and Me-PTCDI supports the model proposed by Scholz and co-workers.[24,25]

Film growth at elevated temperatures causes a significant change in the thin film morphology, with an improvement in crystal quality and size. In addition there is significant elongation of the crystallites at elevated temperatures, although the transition from spherical to elongated features occurs at lower temperatures in the case of Me-PTCDI. These alterations cause a subsequent change in the contributions to the absorption and emission from the various optically active species, although the effects are more pronounced for PTCDA than Me-PTCDI. Growth at elevated temperatures produces an increase in the absorption due to charge-transfer species, and gives rise to an enhancement of the emission, particularly from the high-energy species. In addition, the excimer emission is significantly blue-shifted, indicating that some of the deep traps which can stabilize excimer formation are removed by growth at elevated temperatures. This implies that defect sites play a significant role in the formation of deeply trapped excimer states The enhanced emission manifests itself as a lengthening of the fluorescence decays and hence an increase in the measured lifetimes of the emissive components.

Acknowledgment. This work was supported by the EPSRC, UK. A.J.F. also thanks the Grundy Educational Trust for financial assistance. The authors thank Mr. Richard Sweeney and Mr. Matt Kershaw (Department of Materials, Imperial College London) for assistance with the powder X-ray diffraction measurements, Mr. Stephan Schultes for assisting with the AFM images, and Dr. Sandrine Heutz (Physics Department, University College London) for stimulating discussions and proof reading the manuscript.

References and Notes

(1) Forrest, S. R. *Chem. Rev.* **1997**, *97*, 1793.
(2) Derouiche, H.; Bernede, J. C.; L'Hyver, J. *Dyes Pigm.* **2004**, *63*, 277.
(3) Peumans, P.; Bulovic, V.; Forrest, S. R. *Appl. Phys. Lett.* **2000**, *76*, 2650.
(4) Nakayama, K.; Hiramoto, M.; Yokoyama, M. *J. Appl. Phys.* **2000**, *87*, 3365.
(5) Nakayama, K.; Hiramoto, M.; Yokoyama, M. *Appl. Phys. Lett.* **2000**, *76*, 1194.
(6) Leonhardt, M.; Mager, O.; Port, H. *Chem. Phys. Lett.* **1999**, *313*, 24.
(7) Heutz, S.; Ferguson, A. J.; Rumbles, G.; Jones, T. S. *Org. Electron.* **2002**, *3*, 119.
(8) Mobus, M.; Karl, N.; Kobayashi, T. *J. Cryst. Growth* **1992**, *116*, 495.
(9) Hadicke, E.; Graser, F. *Acta Crystallogr., Sect. C*: *Cryst. Struct. Commun.* **1986**, *42*, 189.
(10) Hoffmann, M. Ph.D. Thesis, Technical University of Dresden, 2000.
(11) Lovinger, A. J.; Forrest, S. R.; Kaplan, M. L.; Schmidt, P. H.; Venkatesan, T. *J. Appl. Phys.* **1984**, *55*, 476.
(12) Yanagi, H.; Toda, Y.; Noguchi, T. *Jpn. J. Appl. Phys., Part 1* **1995**, *34*, 3808.
(13) Friedrich, M.; Himcinschi, C.; Salvan, G.; Anghel, M.; Paraian, A.; Wagner, T.; Kampen, T. U.; Zahn, D. R. T. *Thin Solid Films* **2004**, *455*−*56*, 586.
(14) Bulovic, V.; Burrows, P. E.; Forrest, S. R.; Cronin, J. A.; Thompson, M. E. *Chem. Phys.* **1996**, *210*, 1.
(15) Bulovic, V.; Forrest, S. R. *Chem. Phys.* **1996**, *210*, 13.
(16) Soos, Z. G.; Hennessy, M. H.; Wen, G. *Chem. Phys.* **1998**, *227*, 19.
(17) Hoffmann, M.; Schmidt, K.; Fritz, T.; Hasche, T.; Agranovich, V. M.; Leo, K. *Chem. Phys.* **2000**, *258*, 73.
(18) Hoffmann, M.; Soos, Z. G. *Phys. Rev. B* **2002**, *66*, a024305.
(19) So, F. F.; Forrest, S. R. *Phys. Rev. Lett.* **1991**, *66*, 2649.
(20) Scholz, R.; Kobitski, A. Y.; Kampen, T. U.; Schreiber, M.; Zahn, D. R. T.; Jungnickel, G.; Elstner, M.; Sternberg, M.; Frauenheim, T. *Phys. Rev. B* **2000**, *61*, 13659.
(21) Shen, Z.; Burrows, P. E.; Forrest, S. R.; Ziari, M.; Steier, W. H. *Chem. Phys. Lett.* **1995**, *236*, 129.
(22) Nollau, A.; Hoffmann, M.; Fritz, T.; Leo, K. *Thin Solid Films* **2000**, *368*, 130.
(23) Kobitski, A. Y.; Scholz, R.; Vragovic, I.; Wagner, H. P.; Zahn, D. R. T. *Phys. Rev. B* **2002**, *66*, a153204.
(24) Kobitski, A. Y.; Scholz, R.; Salvan, G.; Kampen, T. U.; Wagner, H. P.; Zahn, D. R. T. *Appl. Surf. Sci.* **2003**, *212*, 428.
(25) Scholz, R.; Kobitski, A. Y.; Vragovic, I.; Wagner, H. P.; Zahn, D. R. T. *Org. Electron.* **2004**, *5*, 99.
(26) Scholz, R.; Schreiber, M.; Vragovic, I.; Kobitski, A. Y.; Wagner, H. P.; Zahn, D. R. T. *J. Lumin.* **2004**, *108*, 121.
(27) Azaroff, L. V.; Kaplow, R.; Kato, N.; Weiss, R. J.; Wilson, A. J. C.; Young, R. A. *X-ray Diffraction*; McGraw-Hill: New York, 1974.
(28) Bailey, J. *J. Chem. Soc. Perkin Trans. 1* **1977**, *1977*, 2047.
(29) Nishimura, H.; Yamaoka, T.; Mizuno, K.; Iemura, M.; Matsui, A. *J. Phys. Soc. Jpn.* **1984**, *53*, 3999.
(30) Pope, M.; Swenberg, C. E. *Electronic Processes in Organic Crystals and Polymers.*; Oxford Science Publications: Oxford, UK, 1999.